Organometallics **2004,** *23,* 2715−2723

Zeolite Activation of Organometallics: Anchoring and Decarbonylation Kinetics of $Mo(CO)_6$ in Dehydrated $Na_{56}Y$ Zeolite

Anthony L. Fernandez,† Jianbin Hao, Roberta L. Parkes, Anthony J. Poë,* and Eduardo J. S. Vichi‡

Lash Miller Chemical Laboratories, University of Toronto, 80 St. George Street, Toronto, Ontario, Canada M5S 3H6

Received January 15, 2004

Quantitative temperature-dependent kinetic studies are reported of thermal reactions of $Mo(CO)_6$ that has been newly encapsulated in the α-cages of a $Na_{56}Y$ zeolite host. Under static vacuum, $Mo(CO)_6$ undergoes *parallel* anchoring and decarbonylation reactions, the latter yielding $(OC)_3Mo-Na_{56}Y$ directly and the former resulting in the development of a characteristic six-band spectrum in the C−O stretching region. Kinetic and spectroscopic evidence was obtained for there being two different forms of $(OC)_3Mo-Na_{56}Y$. The activation parameters are unusual, with very low enthalpies and extremely negative entropies, viz. $\Delta H^{\ddagger} = 40 \pm 3$ kJ mol^{-1} and $\Delta S^{\ddagger} = -185 \pm 9$ J K^{-1} mol^{-1} for anchoring and decarbonylation. This contrasts with the typically high enthalpic and positive entropic factors reported for corresponding CO dissociative reactions in xylene ($\Delta H^{\ddagger} = 133 \pm 6$ kJ mol^{-1} and $\Delta S^{\ddagger} = +28 \pm 16$ J K^{-1} mol^{-1}) or even the quite unusual values $\Delta H^{\ddagger} = 61 \pm 5$ kJ mol^{-1} and $\Delta S^{\ddagger} = -139 \pm 13$ J K^{-1} mol^{-1} reported previously for ^{13}CO exchange in $Mo(CO)_6-Na_{56}Y$. It is concluded that the inner surface of $Na_{56}Y$ provides different activating environments for different reactions, behaving as multidentate anionic “zeolate” nucleophiles, with varying numbers of O^{2-} ions participating in highly ordered transition states. A common intermediate, with three O^{2-} ions participating in the anchoring and decarbonylation process, is proposed, one with two O^{2-} ions being proposed for the ^{13}CO exchange reaction. The importance of temperature-dependent time-resolved infrared spectroscopy in elucidating such intimate mechanistic details is emphasized.

Introduction

The inclusion chemistry of coordination compounds encapsulated in zeolite cavities has been comprehensively reviewed,[1,2] and extensive reports by Ozin,[3] Bein,[1] and others[2,4,5] have provided details of how metal carbonyls are affected structurally and spectroscopically by the encapsulating cavities. Although a huge collection of data for size- and shape-selective intrazeolite catalytic reactions had been accumulated,[6] no detailed kinetic studies of any individual thermal stoichiometric reactions had been reported before 1991. As a result, no precise quantitative information was available regarding the extent to which rates of reaction are affected by the zeolitic environment as compared to the same reactions in homogeneous solution. Without this basic information about individual reactions, no real understanding of the reasons why multistep zeolite-induced catalytic reactions occur can be claimed.

In an attempt to redress the gross imbalance between our knowledge of the more static spectroscopic and structural properties of encapsulated molecules and that of the kinetics of the reactions that they undergo, the first kinetic studies of intrazeolite thermal reactions were undertaken some years ago.[7−9] In view of the substantial spectroscopic and structural knowledge base that was then available[1−5] for archetypal metal carbonyls such as $Mo(CO)_6$, simple substitution reactions of that molecule with ^{13}CO and PMe_3 in the well-defined α-cages of $Na_{56}Y$ were chosen for study.[7−9] The kinetics of these “model” reactions were monitored by transmission infrared spectroscopy, which was made possible

---

* To whom correspondence should be addressed. E-mail: apoe@chem.utoronto.ca.

† Present address: Department of Chemistry, Merrimack College, 315 Turnpike Street, North Andover, MA 01845. E-mail: afernandez@merrimack.edu.

‡ Permanent address: Instituto de Quimica, UNICAMP, C. Postal 6154, 13083-970 Campinas, SP, Brazil. E-mail: vichi@iqm.unicamp.br.

(1) Bein, T., In *Comprehensive Supramolecular Chemistry*; Lehn, J.-M., Atwood, J. L., Davies, J. E. D., MacNicol, D. D., Vögtle, F., Eds.; Pergamon: Oxford, U.K., 1996; Vol. 7, Chapter 20.

(2) Brémard, C. *Coord. Chem. Rev.* **1998**, *178−180*, 1647.

(3) (a) Ozin, G. A.; Gil, C. *Chem. Rev.* **1989**, *89*, 1749. (b) Özkar, S.; Ozin, G. A.; Moller, K.; Bein, T. *J. Am. Chem. Soc.* **1990**, *112*, 9275. (c) Ozin, G. A.; Özkar, S. *Chem. Mater.* **1992**, *4*, 511.

(4) Umemara, Y.; Minai, Y.; Tominaga, T. *J. Phys. Chem. B* **1999**, *103*, 647.

(5) Coddington, J. M.; Howe, R. F.; Yong, Y. S.; Asakura, K.; Iwasawa, Y. *J. Chem. Soc., Faraday Trans.* **1990**, *86*, 1015.

(6) Vaughan, D. E. W. In *Comprehensive Supramolecular Chemistry*; Lehn, J.-M., Atwood, J. L., Davies, J. E. D., MacNicol, D. D., Vögtle, F., Eds.; Pergamon: Oxford, U.K., 1996; Vol. 7, Chapter 13.

(7) Ozin, G. A.; Özkar, S.; Pastore, H. O.; Poë, A. J.; Vichi, E. J. S. *J. Chem. Soc., Chem. Commun.* **1991**, 141.

(8) Pastore, H. O.; Ozin, G. A.; Poë, A. J. *J. Am. Chem. Soc.* **1993**, *115*, 1215.

(9) Ozin, G. A.; Özkar, S.; Pastore, H. O.; Poë, A. J.; Vichi, E. J. S. *ACS Symp. Ser.* **1992**, *No. 499*, 314.

10.1021/om040005v CCC: \$27.50
Publication on Web 04/27/2004

because the intensities of the bands due to the reactants obeyed Beer's law.

Several distinguishing kinetic features were evident for these reactions, but the main one was the ~70 kJ mol^{-1} decrease in activation enthalpy for the exchange reaction with ^{13}CO compared with reactions in solution or in the gas phase.[10] This was offset by a large decrease in the activation entropy, which nevertheless still allowed for an overall acceleration of the rates by a factor of $\sim 10^3$ at 66 °C. This was attributed to stabilization of the transition state for dissociative loss of CO by enthalpically favorable, but entropically unfavorable, interactions of the carbonyl with the extraframework Na^+ ions and/or O^{2-} ions in the cavity walls.[7-9]

Although detailed studies of other aspects of such basic systems have continued to appear in the literature,[11-15] no further kinetic studies have been reported since then.[16] We wish to end this hiatus by reporting kinetic studies of some very basic aspects of the behavior of $Mo(CO)_6$ in $Na_{56}Y$. While some of the recent studies[13,14] have had to do with the formation and characterization of subcarbonyl species, neither of them has described the rates at which the decarbonylation occurs. Nor has any attention been paid to the kinetics of the slow "anchoring" of the $Mo(CO)_6$ that occurs[3] after initial loading of the carbonyl into the α-cavities of the $Na_{56}Y$, and we wish to report the study of the kinetics of these two very fundamental processes.

The spectroscopic basis on which these studies were built was as follows. The infrared spectra of $Mo(CO)_6$ in the presence of CO or PMe_3 indicated that the carbonyl[3b,8] was relatively free to rotate within the α-cage, although the single observed band was very broad compared with that of the carbonyl in solution. This suggested that the oxygen atoms in the CO ligands were each moving in and out of proximity to the highly polarizing Na^+ ions as the carbonyl rotated. The newly encapsulated carbonyl by itself also showed this feature,[3b,9] but on standing at room temperature, its spectrum slowly changed to one showing a total of six bands. This was taken to be indicative of a virtually complete loss of symmetry as a consequence of some sort of anchoring of the formerly rotating $Mo(CO)_6$. This, in turn, must reflect the fundamental details of the equilibrium thermal interaction between this metal carbonyl and the interior of the zeolite. There is some disagreement in the literature about the nature of the anchoring,[2,3b,11a] and it was evidently important to investigate the rates at which it occurs so that some greater understanding of the process might be reached. The relative slowness of the anchoring, and the techniques established by the previous kinetic studies,[7-9] made this possible, and we report here the results of such a study. In comparison with the intrazeolite CO substitution processes,[7-9] a substantially smaller activation enthalpy was observed, and the activation entropy was even more negative. In addition, this anchoring process, rather than preceding decarbonylation, was unexpectedly accompanied by a *simultaneous* decarbonylation to form the previously identified[3b,14,15] subcarbonyl $(OC)_3Mo{-}Na_{56}Y$, the formation of which must therefore be governed by essentially the same distinctive activation parameters as the anchoring process.

Experimental Section

Only a summary of the Experimental Section is provided here, full details being given in the Supporting Information. The high-purity sample of crystalline sodium Y ($Na_{56}Y$; $Na_{56}(AlO_2)_{56}(SiO_2)_{136}(\sim 256\ H_2O)$) was calcined, slurried with NaCl/NaOH, washed and dried as before,[8] and stored at constant humidity. Crystallinity was checked by powder X-ray diffraction.

Each sample of $Na_{56}Y$ for kinetic studies was prepared by pressing the zeolite into a self-supporting wafer. This was then mounted in a steel holder and transferred to the reaction chamber, which was connected to a vacuum line.[17] There it was suitably treated by calcining etc.,[8] and a sample of $Mo(CO)_6$ was added to a sublimation chamber attached by a sidearm to the cell. This chamber was then also evacuated before the main reaction chamber was detached from the vacuum line and transferred to the spectrophotometer. The holder was introduced between the windows of the temperature-controlled IR cell, and baseline spectra were obtained. Loading of the $Mo(CO)_6$ was then accomplished by opening up the cell to the sublimation chamber containing the sample for a few seconds, and a spectrum was then taken. This was repeated until initial absorbances of the main $Mo(CO)_6$ IR band for the kinetic runs were between 1 and 2 units, which corresponds to 1−2 molecules per unit cell (or 8 α-cavities), respectively. Although runs were usually carried out under static vacuum, if a run was to be carried out at some stage under a known atmosphere of CO, the cell had to be reconnected to the vacuum line for addition of the gas before being transferred again to the spectrophotometer.

The temperature controller of the cell was then set to the desired temperature, which was attained after a few minutes. The time-dependent spectra, and absorbance changes at chosen wavenumbers, were then collected automatically so that they could be stored and manipulated as required. The absorbance changes were fitted, as appropriate (see below), to single- or double-exponential functions that provided values of rate constants (k_{obs}) and allowed the derivation of activation parameters by standard Eyring analyses.

Results

Spectroscopic Changes. IR spectra, recorded immediately after the room-temperature sublimation and adsorption of $Mo(CO)_6$ from the vapor phase into the dehydrated $Na_{56}Y$ under vacuum, show a single broad band centered at ~1975 cm^{-1}. In addition there are shoulders at ~2055 and ~1900 cm^{-1} and a weak band at 2123 cm^{-1}, as shown in Figure S1 in the Supporting Information (SI). The half-widths of the main band after room-temperature loading were quite constant at 60−70 cm^{-1}.

---

[10] (a) Howell, J. A. S.; Birkinshaw, P. M. *Chem. Rev.* **1983**, *83*, 557. (b) Angelici, R. J.; Graham, J. R. *J. Am. Chem. Soc.* **1966**, *88*, 3658; *Inorg. Chem.* **1967**, *6*, 2082.

[11] (a) Brémard, C.; Ginestet, G.; Laureyns, J.; Le Maire, M. *J. Am. Chem. Soc.* **1995**, *117*, 9274. (b) Brémard, C., Ginestet, G.; le Maire, M. *J. Am. Chem. Soc.* **1996**, *118*, 12734.

[12] Yang, S.; Navrotsky, A. *Microporous Mesoporous Mater.* **2000**, *37*, 175.

[13] Lim, K. H.; Grey, C. P. *J. Am. Chem. Soc.* **2000**, *122*, 9768.

[14] Okamoto, Y.; Kubota, T. *Microporous Mesoporous Mater.* **2001**, *48*, 301 and references therein.

[15] Yamaguchi, A.; Suzuki, A.; Shido, T.; Inada, Y.; Asakura, K.; Nomura, M.; Iwasawa, Y. *J. Phys. Chem. B* **2002**, *106*, 2415.

[16] (a) Some important kinetic studies of decarbonylation of $Mo(CO)_6$ on alumina surfaces have been reported, however.[16b] (b) Reddy, K. P.; Brown, T. L. *J. Am. Chem. Soc.* **1995**, *117*, 2845.

[17] The cell was designed by Professor G. A. Ozin of this department, and a figure and detailed description are given in ref 8.

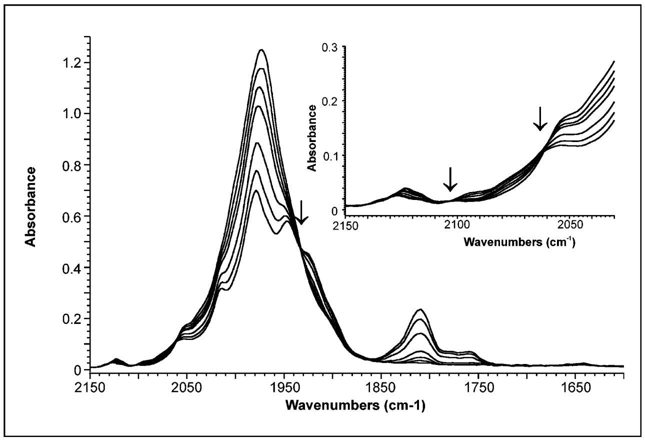

Figure 1. Typical spectroscopic changes during the first stage of reaction at 35 °C while the sharp isosbestic point at 1932 cm^{-1} was evident: i.e., for 90 min or ~85% of the first stage of reaction. The inset shows the presence of two other isosbestic points at 2002 and 2102 cm^{-1}. Spectra were selected to show good separation, ca. 40 spectra being recorded over this time period.

The initially adsorbed $Mo(CO)_6$ underwent clean IR changes on standing under vacuum at ambient temperature, or on heating to defined temperatures between 35 and 85 °C. A typical set of spectra over the initial stage of reaction is shown in Figure 1 for a run at 35 °C. The absorbance of the original band at 1978 cm^{-1} decreases, but the absorbance at 1925 cm^{-1}, on the side of the initial broad band, increases in intensity from the beginning, and the band at 1925 cm^{-1} emerges. These changes give rise to a sharp isosbestic point at ~1930 cm^{-1} which remains sharp for at least 90 min: i.e., for ~85% of the initial reaction (see below). The intensities of the higher energy bands all decrease with time, although a general increase between the shoulder at 2055 cm^{-1} and the weak band at 2123 cm^{-1} results in two more quite sharp isosbestic points, as shown by the insert in Figure 1. The general increase in the intensity in this region usually includes a weak band at 2090 cm^{-1}, but this disappears over the later stages of the reaction. After this initial stage the isosbestic points disappear and the bands slowly decrease in intensity and undergo other small changes, as shown in Figure 2. A final spectrum after 42 h is shown in Figure 3 to consist of six bands at 2127, 2055, 2015, 1979, 1945, and 1927 cm^{-1}.

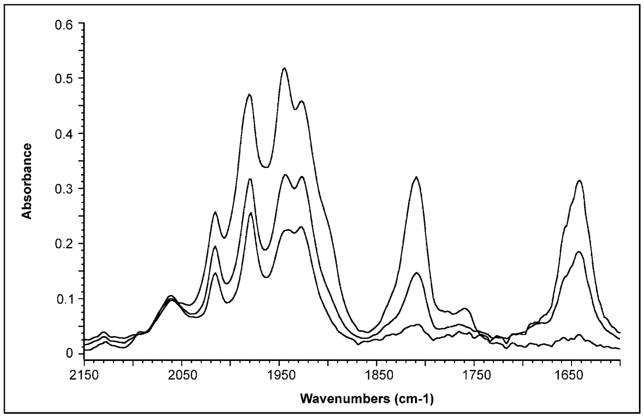

Figure 2. Gradual emergence of the six-band spectrum, over ca. 30 h at 35 °C, after the conclusion of the first stage of reaction and while the band at 1810 cm^{-1} disappears. Note the initially very weak band at 1640 cm^{-1} that grows throughout this period.

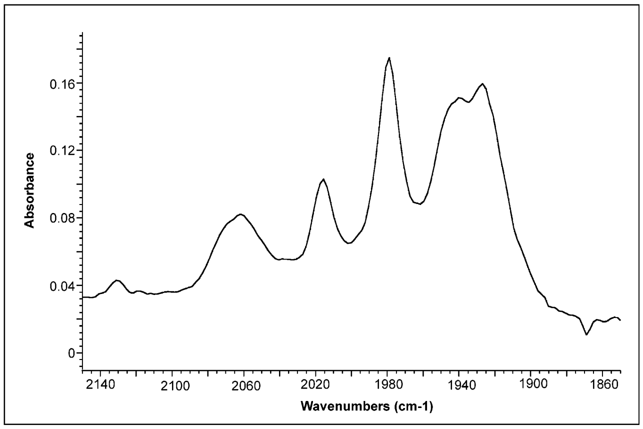

Figure 3. Final six-band spectrum after 42 h at 35 °C when all of the 1810 cm^{-1} band has disappeared.

Coincident with the early spectroscopic changes is the rise (Figure 1) of a band centered at 1810 cm^{-1} with a shoulder at ~1830 cm^{-1} and weak bands at 1780 and 1760 cm^{-1}. This relatively low energy spectroscopic region is characteristic of $Mo(CO)_n$ subcarbonyls with their greater degree of back-bonding to the fewer remaining carbonyl ligands (see Discussion). The intensities in this subcarbonyl region rise to a maximum after ~ 5 h at 35 °C and then decrease and eventually disappear after ~40 h, leaving the six-band spectrum at higher energies clearly apparent for several hours more (Figure 3). An important feature of the later stages of these reactions is evident in Figure 2. It consists of the rise of a band at 1640 cm^{-1}, characteristic of adsorbed water molecules,[18,19] *but this does not begin until well after the isosbestic points have disappeared.* Even the maximum intensity, reached by the time the 1810 cm^{-1} band has disappeared (ca. 30 h at 35 °C), corresponds to less than 10% of complete hydration, i.e., to less than ~3 water molecules per α-cage.[19] This slow incursion of water molecules into the cell, after separation from the vacuum line and over the later stages of reaction, has proved to be unavoidable, but since it is not detected until after the initial reactions are complete, the kinetics of these reactions will not be affected.

Another important feature of the spectroscopic changes is the time dependence of the main band at 1978 cm^{-1}. At lower loading, characterized by initial absorbances of ~1 or less, its intensity continues to decrease slowly and monotonically, although somewhat irregularly, after the initial stage of reaction is complete. However, as the initial loading increases to give an absorbance of ca. 2, the absorbance tends increasingly to go to a minimum, after which it rises and then falls. The absorbance changes in the 1810 cm^{-1} region show no significant dependence on loading, and the existence and positions of the isosbestic points over the early stage of reaction are also unaffected.

Increasing the temperature at which the reactions occur also has little or no effect on the isosbestic points,

---

(18) Bertsch, L.; Habgood, H. W. *Can. J. Chem.* **1963**, *67*, 1621.

(19) Poë, A. J.; Fernandez, A. L. Unpublished observations.

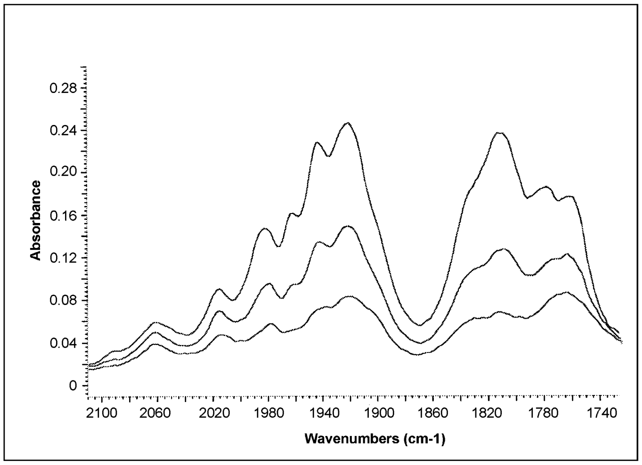

Figure 4. Spectroscopic changes at 75 °C showing the faster decay of the 1810 cm^{-1} band compared with those at 1780 and 1760 cm^{-1}, which become less well resolved.

which remain quite sharp. However, important modifications of the spectroscopic changes become apparent. Over the early stage of reaction, while the isosbestic points are still sharp, the shoulder and low-energy bands close to the growing 1810 cm^{-1} band become relatively much more intense. Associated with this is the fact that the relative intensity of the band at 1923 cm^{-1} becomes higher. However, over the second and much slower stage of reaction, the 1810 cm^{-1} band decreases in intensity more rapidly than the other components in this region, as shown in Figure 4. Thus, the bands in the 1700−1860 cm^{-1} region disappear at rates that are different from each other and from the rates of loss of the six-band spectrum. This occurs in such a way that measurement of the latter in the complete absence of the lower energy bands (as in Figure 3) is no longer possible. A minor feature of these spectroscopic changes is the initial appearance of another weak band at 1960 cm^{-1} in the middle of the “six band” group, but this disappears throughout the slow second stage of the reaction.

Changes in the 1700−1860 cm^{-1} Region after Addition of Carbon Monoxide or Cycloheptatriene. Reactions at 35 and 75 °C were allowed to proceed until the sharpness of the isosbestic points had moderated or until, somewhat later, the absorbances in the 1700−1860 cm^{-1} region had reached their maximum intensity. The reaction cell was then removed from the spectrophotometer and charged either with 650 Torr of CO or with an excess of cycloheptatriene (C_7H_8), and the cell returned to its original temperature. In the former case the bands in the 1700−1860 cm^{-1} region had all disappeared before the measurement of the first spectrum but, as is evident from Figure 5, the spectrum had not reverted to that characteristic of the initially loaded $Mo(CO)_6$. Rather, it had changed to a spectrum similar to that of anchored $Mo(CO)_6$, although the two higher energy bands were not observable due to their masking by the CO bands.

On addition of C_7H_8, the bands in the 1700−1860 cm^{-1} region also disappeared immediately and three new bands at 1946, 1874, and 1823 cm^{-1} appeared. There was no evidence for the band at 1923 cm^{-1}, even as a shoulder to the 1946 cm^{-1} band.

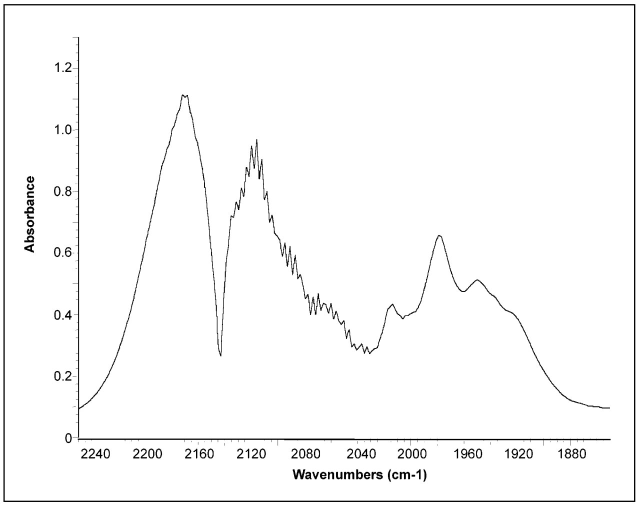

Figure 5. Spectrum following addition of 650 Torr of CO to the cell after the products of the first stage of the reaction had almost completely formed: i.e., soon after the sharpness of the isosbestic points had moderated, the band at 1810 cm^{-1} had completely disappeared, and the band at 1640 cm^{-1} had not yet begun to develop.

Table 1. Rate Constants for Anchoring of $Mo(CO)_6$[a] and Formation of $Mo(CO)_3$[b]

T/°C	$10^4k_{obs}(1978\ cm^{-1})^a/s^{-1}$	$10^4k_{obs}(1810\ cm^{-1})^b/s^{-1}$
35.0	2.56	2.30
35.0	2.61	1.98
35.0	2.32	2.32
48.0	5.33	6.80
48.0	3.60	5.29
56.0	4.31	6.48
66.0	9.51	8.07
75.0	17.9	17.4
75.0	15.9	17.0
75.0	17.0	12.0
75.0	20.8	18.6
85.0	26.2	22.2

[a] From single-exponential analysis of the decreasing absorbance at 1978 cm^{-1} while spectra exhibit a sharp isosbestic point. [b] The rate constant, obtained from the growth of the absorbance at 1810 cm^{-1}, provided by double-exponential analysis of the growth and decay of the absorbance at 1810 cm^{-1}. See the Discussion for assignment of this band to the decarbonylated species.

The Kinetics of Reaction. The clean spectroscopic changes observed throughout the first stage of the observed reactions suggest that rate constants for that step should be readily obtainable. Simple single-exponential (1-e) analysis of the absorbance changes frequently leads to quite good fits of the data, because the second step is appreciably slower than the first. Furthermore, the existence of isosbestic points over a substantial part of the absorbance changes observed in the first stage (Figure 1) suggests that only the reactant $Mo(CO)_6$ and the products of the first stage are present in detectable quantities over that time period. We therefore analyzed the decreasing absorbances observed at 1978 cm^{-1} by 1-e analyses, using only those data, and the rate constants are shown in Table 1. A typically excellent fit of the data is shown in Figure S2. These analyses provide values of both the rate constants and the absorbances at “infinite time”. The latter show that the isosbestic points are evident for ∼85% of the initial reaction, and a large part of the overall absorbance change at this wavenumber occurs during the first

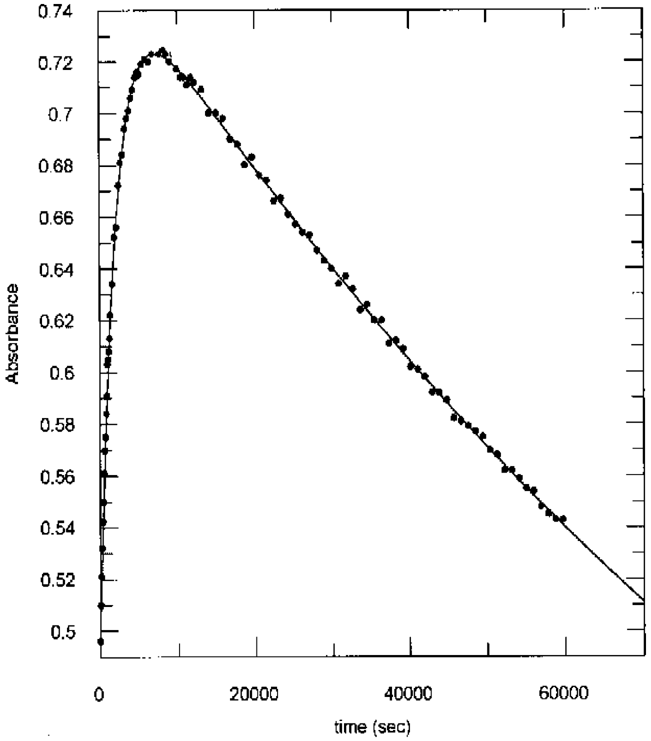

Figure 6. Intensity changes of the band at 1810 cm^{-1} at 66 °C fitted to a double-exponential curve.

stage. This helps explain the appropriateness of these 1-e analyses. Nevertheless, it might be expected that 2-e analyses using data extending over a longer time period might give improved results. This turns out only sometimes to be the case. This is because of the rather haphazard nature of the absorbance changes over the later part of the reactions (see above); i.e., the absorbance changes during the second stage are frequently not simply exponential and a 2-e analysis over a long time period cannot then be successful.

On the other hand, the absorbance changes in the 1700−1860 cm^{-1} region, where the absorbance rises initially and then falls, are not so suitable for 1-e analysis, even when they are restricted to the period during which the isosbestic points are evident. This is because the infinite time absorbances are much larger, and uncertainties in their derivation have a major effect on the rate constants. Also, the absorbance changes over the slower second stage of reaction are more pronounced but they do show good exponential behavior, and 2-e analyses of data over the whole period of reaction show excellent fits to the data, as illustrated in Figure 6. Rate constants obtained in this way for the first stage are also listed in Table 1. It was occasionally necessary, especially for reactions at higher temperatures, for the initial few points to be omitted to allow for adjustment of the cell to the set temperatures. Out of 13 runs for which spectroscopic changes followed the general trend, only one, at 75 °C, was omitted from the Eyring analysis on the grounds that it led to rate constants that were only ca. 50% of those from the other four runs.

The internal agreement of the rate constants can be illustrated by considering the data from the four other runs at 75 °C. The average of $10^4 k_{obs}$ from the four values based on absorbance changes at 1978 cm^{-1} is 17.9 ± 1.1 s^{-1} with an estimated standard error ($\sigma(k_{obs})$) of ±12% for each measurement, while the average from the absorbance changes at 1810 cm^{-1} is 16.3 ± 1.4 s^{-1} with $\sigma(k_{obs}) = \pm 17\%$. The combination of all six values found from the data at 35 °C leads to an average of 2.33 ± 0.09 s^{-1} with $\sigma(k_{obs}) = \pm 10\%$.

Table 2. Activation Parameters for Reactions of $Mo(CO)_6$ in $Na_{56}Y$

	$\Delta H^{\ddagger a}$	$\Delta S^{\ddagger b}$	$\sigma(k_{obs})$/%	ref
anchoring	41.4 ± 3.0	−181 ± 9	±22	this work
deccarbonylation	39.0 ± 2.9	−189 ± 9	±22	this work
av	40 ± 3	−185 ± 9		this work
^{13}CO exchange	61 ± 5	−139 ± 13	±15	8
P-*n*-Bu_3 substitution	133 ± 6^c	+28 ± 16^c		16b

[a] In kJ mol^{-1}. [b] In J K^{-1} mol^{-1}. [c] Calculated from data in ref 16b for CO-dissociative substitution in decalin.

Scheme 1

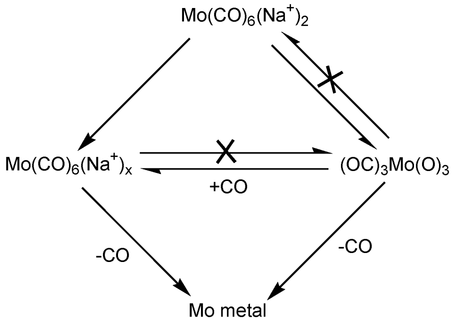

The rate constants can be used to obtain activation parameters by standard Eyring analysis. The rate constants can be treated by assuming they have a constant standard error of measurement, irrespective of the temperature, something that is inherent in all unweighted Eyring analyses, and the activation parameters are given in Table 2. The rate constants obtained by monitoring the absorbance decreases at 1978 cm^{-1}, and concurrent formation of the six-band spectrum of the anchored species, lead to parameters that are essentially identical with those from increasing absorbances at 1810 cm^{-1}, corresponding to the decarbonylation process; therefore, the average values of $\Delta H^\ddagger$ and $\Delta S^\ddagger$ can be taken as satisfactorily precise activation parameters for the observed process. Alternative analyses involving averaging of data at each temperature, with appropriate weighting, again lead to the same values.

Discussion

The spectra obtained immediately after sublimation of the $Mo(CO)_6$ into the zeolite wafer were identical with those reported elsewhere.[3b,8] The subsequent spectroscopic changes can be discussed in terms of the simple picture shown in Scheme 1. The species $Mo(CO)_6(Na^+)_2$ is the initially loaded $Mo(CO)_6$, which is free to rotate in and out between two Na^+ ions in such a way that the C−O stretching band is greatly broadened. $Mo(CO)_6(Na^+)_x$ is a strongly anchored $Mo(CO)_6$ molecule, characterized by a six-band spectrum, and $(OC)_3Mo(O)_3$ is the subcarbonyl, formed directly from $Mo(CO)_6(Na^+)_2$ and in which three facial coordination sites are occupied by three oxide ions from the inner surface of the $Na_{56}Y$.

The isosbestic points observed during the initial stage of reaction, and the fact that the attainment of the six-band spectrum and the growth of the bands in the subcarbonyl region occur simultaneously at identical rates, shows that two parallel reactions are occurring. One path leads to decarbonylation and the other to strong anchoring. Both the anchored species and the subcarbonyl lose CO irreversibly to form Mo metal. However, the subcarbonyl does not revert to unanchored $Mo(CO)_6$ in the presence of CO. Instead, it very rapidly forms $Mo(CO)_6$, which is anchored in essentially the same way as when anchoring occurs directly from unanchored $Mo(CO)_6$.

Six-band spectra of the sort seen here have been reported previously[2,3b] and, as implied above, have been assigned to some sort of anchoring of the $Mo(CO)_6$ within the $Na_{56}Y$ that causes a decrease of the symmetry to C_{2v} or less. However, the exact nature of the anchoring has been disputed. Ozin et al.[3b] originally suggested that the $Mo(CO)_6$ was situated between two sodium ions within the same α-cage, the oxygen atoms of two trans CO ligands being attracted to the sodium ions. The distance between the sodium ions is such that the two CO ligands can be simultaneously bonded in this way, and the maximum loading of two $Mo(CO)_6$ molecules per α-cage is consistent with this. This is analogous to similar suggestions[3a] for the anchoring of molecules such as $CpRh(\text{or Co})(CO)_2$ in $Na_{56}Y$, although in these cases the dimensions of the α-cage were such that the molecules were either anchored via the Cp ring to one sodium ion or anchored to a sodium ion through the two CO ligands.

More recently[2,11a] Brémard et al. have suggested that the most stable anchored form at relatively low loadings involves the positioning of the $Mo(CO)_6$ in a window between two α-cages. This allows for interactions of all the CO ligands with six sodium ions, three in each α-cage as described and illustrated in refs 2 and 11a, so that x in Scheme 1 is 6. At higher loadings anchoring of the "Ozin type" occurs instead, with two $Mo(CO)_6$ molecules in the same α-cage.

The reversible formation of subcarbonyls has also been well established.[20] However, the exact number of CO ligands present, and the question of how many subcarbonyls might successively be formed and detected, were uncertain until Ozin et al. demonstrated[3b] that the major subcarbonyl formed was $Mo(CO)_3$. The Mo atom was bonded to three framework O^{2-} ions that were acting as what was termed a "zeolate" ligand. This assignment was based on spectroscopic analysis of isotopically labeled subcarbonyls and the fact that the subcarbonyl reacted rapidly with several tridentate molecules (L_3) such as tricycloheptatriene to form the expected $(L_3)Mo(CO)_3$ products. Quite recently it has been shown by a temperature-programmed decomposition technique that $Mo(CO)_6$ decomposes to metal atoms via the subcarbonyl $Mo(CO)_3$, which was also believed to have its other three coordination sites occupied by zeolite framework oxygen ions.[14] No other intermediates were detected. Further, in situ time-resolved energy-dispersive X-ray absorption fine structure studies can provide EXAFS spectra at a rate of 1 per second. Iwasawa et al. have used this technique to show that $Mo(CO)_3$ is the only subcarbonyl formed in the thermal decomposition of $Mo(CO)_6$ in the temperature range 127−227 °C and confirmed that the vacant coordination sites are filled with framework oxide ions.[15]

Our spectroscopic and kinetic results provide a detailed picture of both the anchoring and decarbonylation processes. Upon sublimation of the $Mo(CO)_6$ molecules into $Na_{56}Y$ we conclude that they are rapidly distributed throughout the α-cages, where they give rise to the broad band at 1978 cm^{-1} in the C−O stretching region of the IR spectrum. Subsequently, at ambient or higher temperatures, this band is slowly replaced by a six-band spectrum showing peaks ranging from 1923 to 2123 cm^{-1}, and these are characteristic of a low-symmetry environment for anchored $Mo(CO)_6$. Brémard et al.[10a] suggested that this development of the six-band spectrum occurred during a so-called "equilibration period" and was due to the slow diffusion of the $Mo(CO)_6$ in the voids of the crystalline zeolite until it reaches a stable sorption site in a window where it can be anchored and the six-band spectrum is produced: i.e., the development of the six-band spectrum is diffusion controlled. For this reason, Brémard et al. allowed the $Mo(CO)_6$ to equilibrate for 12 h at 0 °C before examination of the anchored species with its six-band spectrum. However, no other similar evidence for slow diffusion into the zeolite has been observed when other carbonyl complexes have been sublimed into $Na_{56}Y$, and we believe our kinetic results are more consistent with slow anchoring and decarbonylation occurring *simultaneously* at virtually the same, or identical, rates.

Thus, the transformation from the essentially single-band to the six-band spectrum is "spectroscopically clean" in that sharp isosbestic points are observed for the major part of the initially observed process. At the same time, and at the same rates, a clear band at 1810 cm^{-1} is observed to grow, and this is accompanied by a weak shoulder on the high-energy side and weak bands at 1780 and 1760 cm^{-1} on the low-energy side (Figure 1). As has been concluded before,[3b,20] the low energy of all these bands suggests that they correspond to subcarbonyl species, and it is therefore clear that the initially observed process involves simultaneous anchoring and decarbonylation.

The intensity of the subcarbonyl group of bands increases with time to a maximum, after which they decrease in intensity and eventually disappear (Figure 6). At lower temperatures there is a residual spectrum comprising the six bands of the low-symmetry anchored species, although that itself disappears eventually. However, as the temperature is increased, the relative rates of disappearance of the six-band spectrum and the subcarbonyl bands change, so that obtaining a six-band spectrum free of residual subcarbonyl bands is no longer possible. The intensity distribution within the isolated six-band spectrum at 35 °C changes slightly from run to run without any particular pattern being evident. However, the actual positions of the bands within the six-band spectrum do not change and we regard the relative intensity changes as a reflection of changes in fine details of the nature of the anchoring (see below).

Some clearer changes in the relative intensities occur with increasing temperature when the 1923 cm^{-1} band and the lower energy 1780 and 1760 cm^{-1} bands become relatively much more intense. This can be attributed to the fact that some of the intensity of the 1923 cm^{-1}

---

[20] E.g.: Abdo, S.; Howe, R. F. *J. Phys. Chem.* **1983**, *87*, 1713.

band is associated with a subcarbonyl species. Ozin et al. assigned bands at 1923, 1794, and 1754 cm^{-1} to the subcarbonyl $(OC)_3Mo-NaY$ (or $(O)_3Mo(CO)_3$) and the higher intensity of the band observed here at 1923 cm^{-1} when the 1780 and 1760 cm^{-1} bands are also present and strong is in agreement with Ozin's observations. However, Ozin et al.[3b] did not report a subcarbonyl band at 1810 cm^{-1} but its presence is clearly evident in our time-dependent spectra, and it can also be ascribed to a subcarbonyl species. It differs from the one characterized by the three bands at 1923, 1780, and 1760 cm^{-1} since, although its rate of formation is the same as that of the other subcarbonyl bands, its rate of disappearance is noticeably faster. It seems probable that a combination of the quite different temperatures (100−150 °C) [3b] at which decarbonylation was carried out elsewhere, and the (unspecified) times before spectra were measured, were such that the 1810 cm^{-1} band had completely disappeared before spectra were taken. In addition, we find that the 1810 cm^{-1} species reacts with CO or cycloheptatriene in exactly the same way as the other subcarbonyl and we believe that the two different subcarbonyls represent slightly different forms of the same zeolate complex $(O)_3Mo(CO)_3$, rather than subcarbonyls with different stoichiometry. The 1810 cm^{-1} band is unlikely to be the only band shown by this second subcarbonyl, and we assume that the other bands are concealed by those of the first. They are formed at the same rate from $Mo(CO)_6$ and do not transform into each other, so that stoichiometries of $(O)_2Mo(CO)_4$ and $(O)Mo(CO)_5$ seem unlikely, as does $(O)_4Mo(CO)_2$. It has also been suggested elsewhere that a single subcarbonyl could be bonded to the interior of NaY in two different ways.[3b] There are now also the other, kinetic, reasons for believing this, namely the different rates at which the 1810 and 1760 cm^{-1} bands disappear.

This brings us to the question of what the detailed nature of the anchoring process actually is. In our view, Ozin-type anchoring to two sodium ions within the same α-cage would involve a simple process whereby any "free" $Mo(CO)_6$ molecules could slip easily between two sodium ions. That would seem unlikely to require any appreciable activation and should be very fast, the anchoring being quite weak. A similar rapid anchoring is apparently observed with the complexes $CpM(CO)_2$ (M = Co, Rh) since no question of slow anchoring was addressed.[3a] The existence of so-called "free" $Mo(CO)_6$, suspended in the center of a cavity without any interaction with the Na^+ ions, is therefore unlikely. The Ozin-type anchoring might be sufficiently weak for the $Mo(CO)_6$ to be quite free to rotate between two Na^+ ions or move between different pairs. It does this in a way that the oxygen atoms of the carbonyl ligands pass in and out of the influence of the polarizing sodium ions, so leading to the broadness of the single band observed in the IR spectrum. On the other hand, the Brémard-type anchoring process would be more complex and would certainly be unfavorable entropically. We believe that our kinetic data support this assignment.

Scheme 2

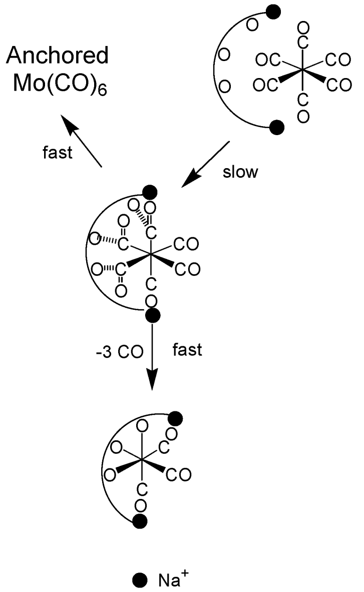

Scheme 3

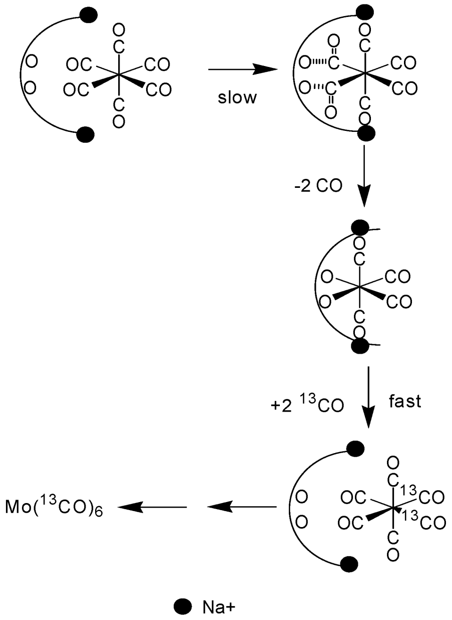

The kinetics of this anchoring process, and of the associated decarbonylation, are generally well behaved and satisfactorily reproducible. The rate constants obtained from the formation of the anchored $Mo(CO)_6$ species and the decarbonylated $(O)_3Mo(CO)_3$ are indistinguishable, and the activation parameters (Table 2) are defined by having a very low value of the activation enthalpy and a very negative and unfavorable value for the activation entropy. (This is true even when data from all runs were included indiscriminately and all methods of derivation of rate constants were accepted.) This contrasts with the values for the intrazeolite CO exchange reaction, which are considerably less favorable enthalpically and considerably less unfavorable entropically, while the latter are again considerably less favorable enthalpically and less unfavorable entropically than the reactions in homogeneous solution.[10] We regard this as being explicable on the basis of Schemes2 and 3. For decarbonylation we propose that three oxide ions displace three *fac* CO ligands by initial coordination to their carbon atoms, as shown in Scheme 2. Some participation by attachment of sodium ions to the O atoms of CO ligands might also occur. This process would be entropically very unfavorable, due to the essentially simultaneous coordination required by the rigid assembly of the three oxide ions, but this would be offset by less unfavorable enthalpy factors associated with the greater degree of bond-making involved. Attack at the carbon atoms of metal carbonyls by hard nucleophiles, including oxygen donors, is very well documented;[10a] thus, this process has sound precedents. This implies that decarbonylation occurs in *one rate-determining step* and not via less decarbonylated species such as $(O)Mo(CO)_5$ and $(O)_2Mo(CO)_4$. For simplicity, Scheme 2 implies that formation of the intermediate $(OOC)_3Mo(CO)_3(Na^+)_n$ occurs within an α-cage but might equally well occur within a window between two α-cages and, although n is indicated to be 2 in Scheme 2, it could be much less well defined. These considerations provide a possible explanation for why the rates of formation of the anchored and decarbonylated products are the same and why the decarbonylated species is also probably generated in the windows between two α-cages (see below). If, as indicated in Scheme 2, the $(OOC)_3Mo(CO)_3(Na^+)_n$ could proceed further along the reaction coordinate to form *either* the anchored or decarbonylated species, then there would be a common rate-determining step for forming the two products and their identical rates of formation would not be coincidental. The relative concentrations of these products would, however, be determined by the relative rates of the two possible reactions of the $(OOC)_3Mo(CO)_3(Na^+)_n$ intermediate. These in turn would be governed by the relative ease of breaking the Mo−COO bonds, as opposed to forming more bonds between the Na^+ ions and the oxygen atoms of coordinated CO ligands.

Scheme 3 provides a possible explanation for the higher value of $\Delta H^‡$, and less unfavorable value of $\Delta S^‡$, for the ^{13}CO exchange reactions. The attack by only two oxide ions at the carbon atoms of two CO ligands would, by contrast to the decarbonylation process, be less entropically difficult but correspondingly less favorable enthalpically.

The rapid diffusion of the $Mo(CO)_6$ molecules through the zeolite must involve passage through the windows where the $Mo(CO)_6$ eventually becomes anchored. The reason diffusion is so much more rapid than anchoring is, we believe, a function of the low probability of the anchoring process. This requires a rather precise positioning of the $Mo(CO)_6$ molecules relative to framework oxide ions. This gives the $Mo(CO)_6$ a chance to diffuse rapidly through the windows instead of being eventually captured by the Na^+ ions. In other words, the translational motion of the $Mo(CO)_6$ can compete successfully with the precise rotational movements needed to lead it to a position suitable for anchoring. The enthalpic barrier involved in anchoring can be accounted for if the decarbonylation and anchoring occur via slow formation of the same intermediate, as indicated in Scheme 2.

The rapid reaction of $(O)_3Mo(CO)_3$ with cycloheptatriene is as expected,[3b] but the equally rapid reaction with CO does not return to nonanchored, freely rotating $Mo(CO)_6$. Instead, it returns to a Brémard-type anchored form. This has implications regarding the site at which the $Mo(CO)_3$ is bound. If it were bound in the α-cage itself, then reaction with CO would more likely form the relatively free form of the $Mo(CO)_6$, which would then have to undergo slow anchoring. It seems therefore that the $Mo(CO)_3$ has to be bound in the vicinity of a 12-ring window, as suggested above, so that the anchored form can be produced directly on reaction with CO.

The kinetics of loss of the anchored and decarbonylated species are not so clearly defined. The loss of the anchored species depends on the exact loading of the $Mo(CO)_6$, and the absorbance changes are irregular and not susceptible to kinetic analysis. Although the decomposition of $(OC)_3Mo(O)_3$ appears to be fairly normal in terms of the monotonic absorbance decreases, the rate constants obtained do not show reproducibility or proper Eyring behavior. There are two possible reasons for these observations. Decomposition is inevitably accompanied by formation of naked Mo atoms, and this along with the growing presence of water molecules over these later stages of reaction (indicated by the IR band at 1640 cm^{-1}) could cause abnormal kinetic behavior. The appearance of the water molecules is shown spectroscopically to begin *after* the first stage of reaction, anchoring and decarbonylation, is complete. Similarly, the formation of naked Mo atoms does not occur until the first stage is essentially over, due to the small overlap of the first and subsequent stages of reaction. The influence of the water molecules or Mo atoms on the kinetics of the first stage is therefore likely to be minimal, although they might contribute to the relatively high standard error of measurement observed.

Finally, the following question has to be asked: why does the ^{13}CO exchange reaction, which is slightly slower than the anchoring/decarbonylation reaction, not proceed via the decarbonylation path, i.e., via formation of the $(OC)_3Mo(O)_3$, which would react rapidly with ^{13}CO? This is probably another example of the dependence of such rates on the details of the environment in which they occur.[8] Although the ^{13}CO exchange reaction is known to be progressively retarded by the presence of increasing partial pressures of the ^{13}CO, it must be that the anchoring process is even more retarded.[21]

Summary

Decarbonylation and anchoring of $Mo(CO)_6$, after sublimation into the α-cages of $Na_{56}Y$, occur at essentially identical rates, probably via the common intermediate $(OOC)_3Mo(CO)_3(Na^+)_n$, in which the second oxygen atom in each COO group is one shared between a CO ligand in the intermediate and the inner surface of a 12-ring window. These reactions are clean and kinetically well defined. Eyring analysis of the data shows the rate-determining process to be entropically much more difficult, but enthalpically much more facile, than that involved in the ^{13}CO exchange with $Mo(^{12}CO)_6$.

The decarbonylation process is strongly indicated to involve formation of the complex $(OC)_3Mo(O)_3$, where the coordinating “zeolate” ligand $(O)_3$ is a triangular group of three oxide ions. The observation of a new band characteristic of a different tricarbonyl species indicates that the $(OC)_3Mo(O)_3$ may exist in more than one

---

[21] Initial attempts to study the anchoring process under an atmosphere of CO suggested that the processes occurring are more complex than expected, and further study is needed to elucidate these.

environment, depending on the temperature of its generation. The time-dependent IR spectra show clearly that the decarbonylated species are formed directly from $Mo(CO)_6$, and not via less decarbonylated species.

Subsequent reactions of the anchored and decarbonylated species are not kinetically well defined, probably because they lead directly to naked Mo atoms and because water molecules diffuse into the system at the same time.

These results confirm that time-resolved spectroscopy of intrazeolite reactions of organometallics, coupled with the derivation of activation parameters, provides a very powerful tool in the elucidation of fine details of those reactions.

Acknowledgment. We gratefully acknowledge the Petroleum Research Fund, administered by the American Chemical Society, and the Natural Sciences and Engineering Research Council of Canada for financial support. E.J.S.V. is grateful for financial support from the FAPESP during his sabbatical leave and to CNPq for support via the PRONEX project.

Supporting Information Available: Text giving details of the syntheses and experimental procedures, and Figures S1 and S2, detailed in the text. This material is available free of charge via the Internet at http://pubs.acs.org.

OM040005V